Fluid Dynamics & Materials Processing FDMP, vol.16, no.1, pp.31-40, 2020

Numerical Study on Aerodynamic Performance of High-Speed Pantograph with Double Strips

Zhiyuan Dai[1], Tian Li[1,*], Weihua Zhang[1] and Jiye Zhang[1]

Abstract: Pantograph is a critical component of the high-speed train. It collects power through contact with catenary, which significantly affects the running safety of the train. Pantograph with double collector strips is one common type. The aerodynamic performance of the collector strips may affect the current collection of the pantograph. In this study, the aerodynamic performance of the pantograph with double strips is investigated. The numerical results are consistent with the experimental ones. The error in the aerodynamic drag force of the pantograph between numerical and experimental results is less than 5%. Three different conditions of the strips are studied, including the front strip, the rear strip, and the double strips. Results show that the presence of the front strip will affect the lift force of the rear strip, and reduce the resistance of the rear strip under the opening condition. Meanwhile, the rear strip has few effects on the front strip under the opening operation condition. The law of the resistance for the interaction between two strips under the closing condition is similar to the opening one.

Keywords: Pantograph, double strip, train aerodynamics, numerical simulation.

1 Introduction

In general, high-speed trains are driven by electricity, and the electric power is sourced from the catenary through the pantograph. Therefore, the pantograph is a key component of the high-speed train. It collects power through contact with catenary, which significantly affects the running safety of train [Raghunathan, Kim and Setoguchi (2002); Zhou (2013)]. It is of considerable significance to study the aerodynamic performance of the pantograph to optimize its structure, improve the control technology. Pantograph with double collector strips is one common type. The strip has a great influence on the aerodynamic performance of the widely used double strip pantographs. The lift force of the strip is an important component of the lift force of the pantograph head. Therefore, the research on the aerodynamic performance of the pantograph strips is particularly important and urgent.

The pantograph is a structure installed on the top of high-speed trains. Its research method is similar to high-speed trains, including the theoretical study, numerical simulation, wind tunnel test, and full-scale test. Theoretical study obtains the results by establishing simplified models and governing equations [Schetz (2003)]. Wind tunnel test

[1] State-key Laboratory of Traction Power, Southwest Jiaotong University, Chengdu, China.

[*] Corresponding Author: Tian Li. Email: litian2008@home.swjtu.edu.cn.

Received: 18 June 2019; Accepted: 25 July 2019.

and full-scale test are expensive. Therefore, numerical simulation has become an effective and valid tool to study train aerodynamics. Researchers have conducted studies on the coupling of pantograph-catenary system. Lee et al. [Lee, Kim, Paik et al. (2012)] studied the design optimization of a pantograph for trains using a finite element method, and the improvement of the current collection was studied and verified. Zhou et al. [Zhou, Zhang and Li (2011)], Antunes et al. [Antunes, Mosca and Ambrosio (2012)] and Zhao et al. [Zhao, Liu and Zhang (2009)] investigated the dynamic characteristics of pantograph-catenary system and the influence of the vibration that caused by the front pantograph on the rear pantograph based on finite element models. Yang et al. [Yang, Jiang and Meng (2012); Ito (2000)] carried out the numerical simulation of pantographs under the opening and closing conditions and analyzed the flow field around and aerodynamic performance of the pantograph. Moreover, the uplift force model was established to calculate the uplift force of pantograph under opening and closing operation conditions by Li et al. [Li, Zhou and Zhang (2013)]. The aerodynamic forces of pantograph fixed on high-speed trains were studied [Liu, Deng, Zheng et al. (2013); Hara, Tanaka, Ohtake et al. (2009)]. The result shows that the resistance of pantographs accounted for 8% to 14% of the whole train. Zhang et al. [Zhang, Zhang, Li et al. (2017)] compared and analyzed the influence of different installation positions of the pantograph on the aerodynamic performance of the high-speed trains. It was found that the installation position had little influence on the head car and had a large effect on the tail car. Iglesias et al. [Iglesias, Thompson, Smith et al. (2016); Iglesias, Thompson and Smith (2017)] analyzed the aerodynamic noise from pantograph through wind tunnel test and numerical simulation and assessed the noise directivity and the speed dependence. The result shows that inflow speed has a large effect on the noise radiation; Pombo et al. [Pombo, Ambrósio, Pereira et al. (2009)] investigated the aerodynamic performance of the pantograph under crosswind conditions, and carried out experimental verification; The unsteady aerodynamic characteristics of the high-speed train pantograph was studied [Guo, Yao, Liu et al. (2017)], and the result shows that the detached eddy significantly affected the aerodynamic lift coefficient of pantographs under presence or absence of crosswind. Sun et al. [Sun and Han (2018); Yao, Guo, Yao et al. (2012)] studied the unsteady resistance and uplift performance under the opening and closing conditions. Results showed that the uplift fluctuations of pantograph under opening conditions were larger than the closing condition.

Up to now, the researches on the pantograph mainly includes the pantograph-catenary dynamic, the aerodynamic noise, and the aerodynamic performances. However, there is a little study on the aerodynamic performance of the strip for the double strip pantographs.

The uplift force of the strip is a necessary part of raising the collector head. It will lead to the generation of the arc if the uplift is too large or too poor. Therefore, it is essential to conduct researches on the strip fixed on the pantograph. This paper establishes three different conditions of the strips to study the aerodynamic characteristics of strips.

2 Governing equation

In computational fluid dynamics (CFD), it is assumed that the fluid satisfies the continuity hypothesis, also satisfies the conservation of energy, and momentum.

Equations corresponding to the three laws are the conservation equations of mass, energy and momentum. Three equations have similarities in mathematical form, and the general governing equation can be obtained by substituting the similar variable with $\boldsymbol{\Phi}$:

$$\frac{\partial \rho \boldsymbol{\Phi}}{\partial t} + \mathrm{div}(\rho u \boldsymbol{\Phi}) = \mathrm{div}(\boldsymbol{\Gamma} \mathrm{grad} \boldsymbol{\Phi}) + \boldsymbol{S}. \tag{1}$$

where ρ is the air density, u is the flow field velocity vector, $\boldsymbol{\Phi}$ is the flow field flux, $\boldsymbol{\Gamma}$ is the diffusion coefficient, $\boldsymbol{S}$ is the source term.

When the train's running speed is lower than 360 km/h, the airflow can be considered as the incompressible and steady flow. In this study, three-dimensional transient incompressible Reynolds average Navier-Stokes and *k-ω SST* (Shear Stress Transport) two-equation turbulence model can be used to solve the governing equations [Li, Zhang and Zhang (2019); Li, Hemida, Zhang et al. (2018)].

3 Computational information

3.1 Single and double strip model

A real pantograph model is used to study the aerodynamic characteristics of strips. Three different conditions of the strips are studied, including the front strip, the rear strip and double strips. Three different models are established. The first one is the front strip (F-strip) pantograph, which only remains the front strip (under the opening condition), as shown in Fig. 1(a). The corresponding pantograph is called F-pantograph. The second one is the rear strip (R-strip) pantograph, which only remains the rear strip (under the opening conditions), as shown in Fig. 1(b). The corresponding pantograph is called R-pantograph. The last one is the double strip (D-strip) pantograph, which has both front and rear strips, as shown in Fig. 1(c). The corresponding pantograph is called D-pantograph. Fig. 1(d) shows the details of the pantograph, including upper arm, lower arm, guide, coupling rod lifting control isolator and collector head.

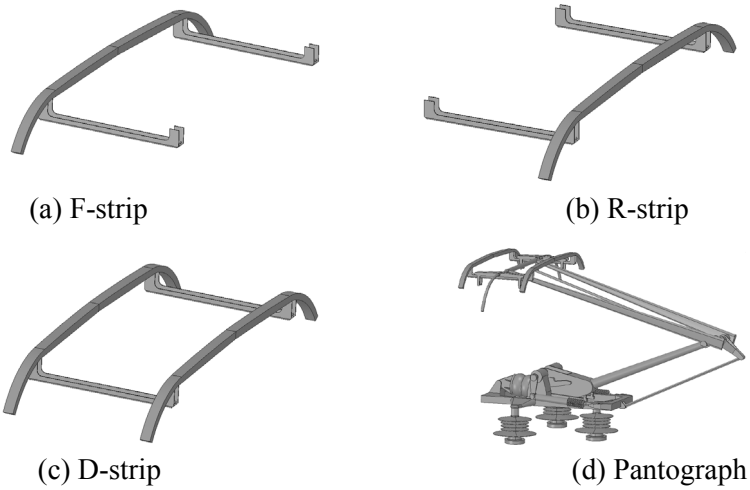

(a) F-strip (b) R-strip

(c) D-strip (d) Pantograph

Figure 1: Model of pantograph and strips

3.2 Computational domain and boundary condition

The computational domain is established as shown in Fig. 2, and a boss is installed on the ground to simulate the roof of the train. The distance between the pantograph and the inlet boundary is 8 m, and the pantograph is 10.8 m far from the outlet boundary.

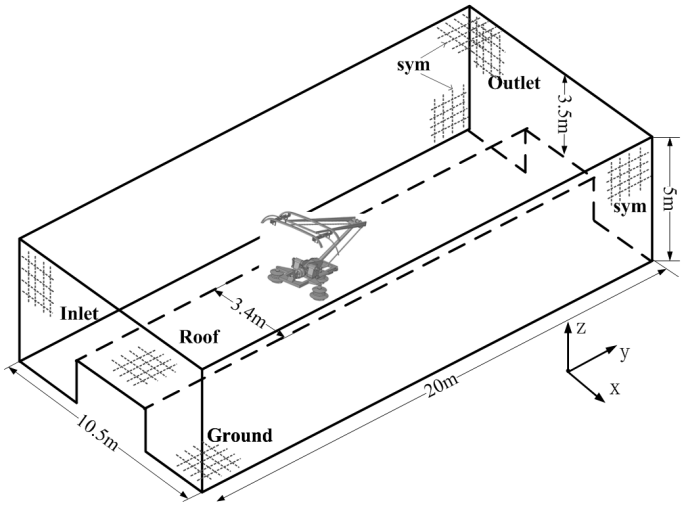

Figure 2: Computational domain

"Inlet" is set as "velocity-inlet" under the opening condition, and the speed is 97.22 m/s. "Outlet" is set as "pressure-outlet", and the pressure is 0. The boundary conditions under the closing conditions are opposite. The sides and top of the computational domain are set as "symmetry". "Roof" is set as a no-slip wall. The ground is set as a slip wall, and the slip velocity is 97.22 m/s.

3.3 Grid Independence test

Three different grids are generated with different sizes, as shown in Tab. 1. The base sizes of the grids Mesh1, Mesh2 and Mesh3 are 260 mm, 200 mm and 180 mm, respectively, and the base size is the largest size of the mesh. The number of the boundary layers is 18. The height of the first boundary layer is 0.01 mm, and growth ratio is 1.2. Tab. 1 gives the numerical results calculated by FLUENT.

Table 1: Results of numerical simulation

Conditions	Basic size(mm)	Number of grids	Lift force of strip(N)	Resistance of strip(N)	Resistance of pantograph(N)
Mesh1	260	29480000	7.15	596.69	1071.76
Mesh2	200	43780000	11.34	626.05	1111.58
Mesh3	180	53800000	13.88	644.81	1114.31

The accuracy of the numerical simulation is improved with the increase of grids. It can be seen from Tab.1 that the relative error between Mesh1 and the other two sets of grids is larger, and the relative error between Mesh2 and Mesh3 is smaller. Therefore, the accuracy of Mesh2 satisfies the calculation requirements. The grid at the cross-section x=0 m is shown in Fig. 3.

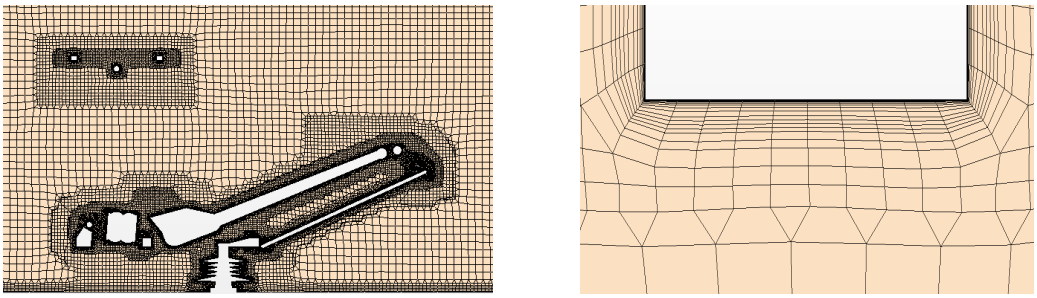

(a) Grid around the lower arm (b) Boundary layer

Figure 3: Grid around the pantograph at the cross-section x=0 m

4 Validation

The numerical results are compared with the experimental results to validate the accuracy of the numerical simulation, as shown in Tab. 2. The experimental data was obtained using the wind tunnel test for a pantograph carried out in a high-speed wind tunnel of China Aerodynamics Research and Development Center. The height of the pantograph is 1.65 m, and the running speed is 350 km/h.

Table 2: Comparison of the resistance between numerical and experimental results

Conditions	Numerical result (N)	Experimental result (N)	Relative error
Opening operation	2900.8	3048.8	4.86%
Closed operation	2826.6	2948.3	4.13%

It can be seen from Tab. 2 that the error of the resistances obtained by numerical simulation and the experimental data are very small, all within 5%, and the resistances obtained using the wind tunnel test are larger than numerical ones under both opening and closing operation conditions. This is because some small parts of the pantograph are omitted to improve the quality of the grids in the numerical simulation. In all, the relative error between results obtained by the numerical simulation and wind tunnel test is small, indicating the accuracy of the computational domain, boundary, mesh, and solving method.

5 Results

The aerodynamic performances of the strips under different conditions are numerically simulated. In the following, the aerodynamic characteristics of the strips are discussed in terms of the aerodynamic forces and flow field around the strips.

5.1 Aerodynamic forces

The mutual influence on the aerodynamic forces between two strips for different types of pantographs is studied. The lift force and resistance of the F-strip and the R-strip are shown in Tab. 3.

Table 3: Aerodynamics forces of strips

	D-pantograph		F-pantograph		R-pantograph	
	Opening condition	Closing condition	Opening condition	Closing condition	Opening condition	Closing condition
Lift force of F-strip(N)	-0.29	-12.26	-0.71	-1.55	--	--
Lift force of R-strip (N)	20.10	-8.92	--	--	8.46	-8.25
Lift force of strips (N)	11.34	-22.52	-4.25	-10.55	-6.92	-4.89
Resistance of F-strip (N)	387.65	-230.47	396.69	-346.03	--	--
Resistance of R-strip (N)	226.73	-365.48	--	--	370.87	-367.81
Resistance of strips (N)	634.05	-615.24	414.34	-364.78	389.89	-384.88

It can be seen from Tab. 3 that the lift force of the strip for D-pantograph is positive in the opening condition, and the R-strip provides a majority of the lift force. By comparing with the F-pantograph and D-pantograph, F-strip in the two pantographs has almost the same lift force, indicating that R-strip has few impacts on the F-strip under the opening condition. Comparing with the R-strip of the R-pantograph and D-pantograph, the lift force of the R-strip for R-pantograph is reduced by 12 N, indicating that F-strip has a greater influence on the lift force of the R-strip under the opening condition.

Under the closing condition, both strips of the D-pantograph show the negative lift force, and the F-strip gives a slightly larger negative lift force than that of the R-strip. By comparing with the R-pantograph and D-pantograph, R-strip in the two conditions has the same negative lift force, indicating that F-strip has few impacts on R-strip under the closing condition. Comparing with the F-strip of the F-pantograph and D-pantograph, negative lift force of the F-strip for F-pantograph is reduced by 11 N, that is, the lift force increases 11 N, indicating that R-strip has a greater influence on the lift force of the F-strip under the closing condition.

The resistances of the F-strip for the F-pantograph and D-pantograph are close to each other under the opening condition, and resistance of the R-strip for the R-pantograph is about 150 N larger than that for the D-pantograph. Under the closing condition, the resistance of the R-strip for the R-pantograph and D-pantograph are close to each other, and the resistance of the F-strip for the F-pantograph is about 110 N larger than that for the D-pantograph. The strip ahead resists partial incoming airflow under both opening and closing condition, which leads to the reduction in the resistance of the strip behind.

5.2 Flow field around strips

In order to analyze the aerodynamic forces of the strips, the flow field around the strips is given in this section.

Take the velocity distribution of the strips at the cross-section x=0 m under the opening condition, for example, Figs. 4(a)-4(c) shows the velocity distribution of the D-pantograph, F-pantograph, and R-pantograph, respectively.

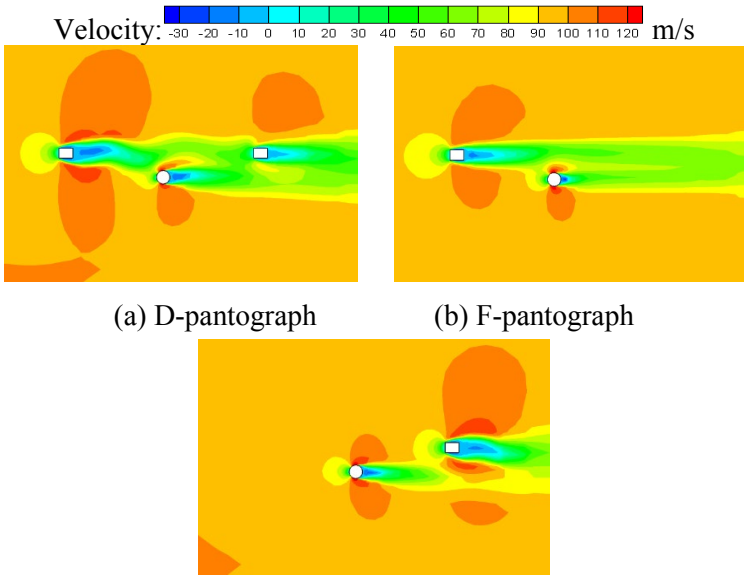

(a) D-pantograph (b) F-pantograph

(c) R-pantograph

Figure 4: Velocity distribution of the strips

It can be seen from Fig. 4(a) that the difference of airflow velocity between the upper and lower surfaces of the F-strip is small, and consequently, the difference of the negative pressure generated on the upper and lower surfaces of the strip is also small. Therefore, the lift force of the F-strip for the D-pantograph is about 0. For the R-strip, the airflow velocity above the strip is larger than that on the lower surface of the strip due to the interference of the tube in the presence of the wake flow. A pressure difference is generated between the upper and lower surfaces. Therefore, the R-strip shows a positive lift force. Comparing Fig. 4(a) with Fig. 4(b), the velocity distribution of the F-strips for two pantographs is similar, and the lift force of the F-strip for the F-pantograph is consistent with the lift force of the F-strip for the D-pantograph. The presence of the R-strip has little effect on the aerodynamic performance of the F-strip. It can be seen in comparison with Fig. 4(a) and Fig. 4(c) that the flow around the R-strip changes greatly, the airflow directly rushes on the R-strip without the blockage of the F-strip. For the R-strip, the velocity above and below the strip increases, however, the velocity below the strip shows a larger increment, therefore, the negative pressure difference between the upper and lower surfaces of R-strip decreases, and so does the lift force.

Under the opening condition, Figs. 5(a)-5(c) shows the velocity distribution around the strips of the D-pantograph, F-pantograph, and R-pantograph, respectively.

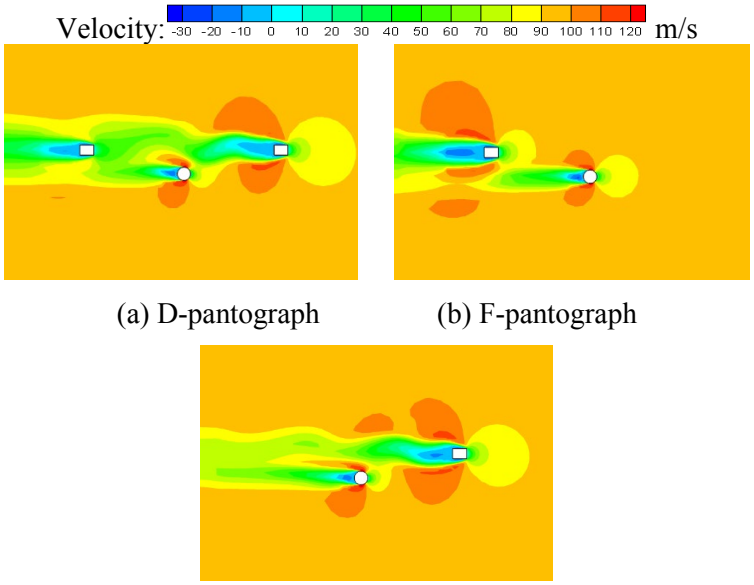

(a) D-pantograph (b) F-pantograph

(c) R-pantograph

Figure 5: Velocity distribution of the strips

The closing conditions differ from the opening conditions in that the airflow velocity around strips is lower than the opening conditions because of the upper arm and other components. The difference of the airflow velocity between the opening and closing conditions leads to the influence of the F-strip on the R-strip under opening condition is greater than the influence of the R-strip on the F-strip under closing condition. It can be seen from Fig. 5(a) that the airflow velocity below the R-strip is larger than that above, the R-strip shows negative lift force. It can be seen in comparison with Fig. 5(a) and Fig. 5(b), the flow around the F-strip changes greatly, airflow directly rushes on the F-strip without the blockage of the R-strip. For the F-strip, the velocity above the strip increases greatly, therefore, the negative pressure difference between the upper and lower surface is smaller, and the lift force of the F-strip is reduced. Comparing Fig. 5(a) with Fig. 5(c), the velocity distribution for the R-strips for two pantographs is similar, and the lift force of the R-strip for the R-pantograph is consistent with the lift force of the R-strip for the D-pantograph. The presence of the F-strip has little effect on the R-strip.

6 Conclusions

The flow around the D-pantograph, F-pantograph and, R-pantograph under the opening and closing conditions are numerically simulated. The interaction of the aerodynamic performance between F-strip and R-strip is studied. The main conclusions are as follows:

(1) Reynolds average Navier-Stokes and the k-ω SST two-equation turbulence model can reproduce the aerodynamic forces accurately in comparison with the wind tunnel experimental data.

(2) The strip ahead resists partial incoming airflow under both opening and closing condition, which leads to the reduction in the resistance of the strip behind.

(3) The presence of the front strip will affect the lift force of the rear strip. Meanwhile, the rear strip has few effects on the front strip under both opening operation condition.

Acknowledgement: This work was supported by Sichuan Science and Technology Program (No. 2019YJ0227), China Postdoctoral Science Foundation (No. 2019M663550), Self-determined Project of State Key Laboratory of Traction Power (2019TPL_T02) and the National Key Research and Development Program of China (2018YFF0215602).

Conflicts of Interest: The authors declare that they have no conflicts of interest to report regarding the present study.

References

Raghunathan, R. S.; Kim, H. D.; Setoguchi, T. (2002): Aerodynamics of high-speed railway train. *Progress in Aerospace Sciences*, vol. 38, no. 6, pp. 469-514.

Zhou, N. (2013)**:** *Investigation on Dynamic Behavior of Pantograph and Catenary System for the Running Speed of 350 km/H or Above (Ph.D. Thesis)*. Southwest Jiaotong University.

Schetz, J. A. (2003): Aerodynamic of high-speed trains. *Advances in Mechanicals*, vol. 33, no. 3, pp. 404-423.

Lee, H. J.; Kim, Y. G.; Paik, J. S.; Park, T. W. (2012): Performance evaluation and design optimization using differential evolutionary algorithm of the pantograph for the high-speed train. *Journal of Mechanical Science & Technology*, vol. 26, no. 10, pp. 3253-3260.

Zhou, N.; Zhang, W. H.; Li, R. P. (2011): Dynamic performance of a pantograph catenary system with the consideration of the appearance characteristics of contact surfaces. *Journal of Zhejiang University-Science A: Applied Physics & Engineering*, vol. 12, no. 12, pp. 913-920.

Antunes, P.; Mosca, A.; Ambrosio, J.; Pombo, J. (2012): Development of a computational tool for the dynamic analysis of the pantograph catenary interaction for high-speed trains. https://dx.doi.org/10.4203/ccp.99.129.

Zhao, F.; Liu, Z. G.; Zhang, X. X. (2012): Simulation of high-speed pantograph-catenary system dynamic performance based on finite element model. *Journal of the China Railway Society*, vol. 34, no. 8. pp. 33-38.

Yang, J. M.; Jiang, X.; Meng, Q. (2012): Fluent based high speed pantograph line running around flow field numerical simulation. *Modern Machinery*, vol. 38, no. 3, pp. 34-36.

Ito, M. (2000): Improvement to the aerodynamic characteristics of Shinkansen rolling stock. *Journal of Rail and Rapid Transit*, vol. 214, no. 3, pp. 135-143.

Li, R. P.; Zhou, N.; Zhang, W. H. (2012): Calculation and analysis of aerodynamic uplift force. *Journal of the China Railway Society*, vol. 34, no. 8, pp. 26-32.

Liu, X.; Deng, J.; Zheng, Y.; Pan, G. F. (2013): Impact of aerodynamics of pantograph of a high-speed train on pantograph-catenary current collection. *Journal of Zhejiang University (Engineering Science)*, vol. 47, no. 3, pp. 558-564.

Hara, N.; Tanaka, K.; Ohtake, H.; Wang, O. (2009): Development of a flying robot with a pantograph-based variable wing mechanism. *IEEE International Conference on Robotics and Automation*, vol. 25, no. 1, pp. 79-87.

Zhang, L.; Zhang, J.; Li, T.; Zhang, W. H. (2017): Influence of pantograph fixing position on aerodynamic characteristics of high-speed trains. *Journal of Modern Transportation*, vol. 25, no. 1, pp. 34-39.

Iglesias, E. L.; Thompson, D. J.; Smith, M.; Yamazaki, N. (2016): Anechoic wind tunnel tests on high-speed train bogie aerodynamic noise. *International Journal of Rail Transportation*, vol. 5, no. 2, pp. 87-109.

Iglesias, E. L.; Thompson, D. J.; Smith, M. (2017): Component-based model to predict aerodynamic noise from high-speed train pantographs. *Journal of Sound and Vibration*, vol. 394, pp. 280-305.

Pombo, J.; Ambrósio, J.; Pereira, M.; Rauter, F.; Collina, A. et al. (2009): Influence of the aerodynamic forces on the pantograph-catenary system for high-speed trains. *Vehicle System Dynamics*, vol. 47, no. 11, pp. 1327-1347.

Guo, D. L.; Yao, S. B.; Liu, C. W.; Yang, G. W. (2017): Unsteady aerodynamic characteristics of high-speed pantograph. *Journal of the China Railway Society*, vol. 34, no. 11, pp. 16-21.

Sun, X. Q.; Han, X. (2018): Numerical modeling and investigation on aerodynamic noise characteristics of pantographs in high-speed trains. *Complexity*, vol. 25, no. 6, pp. 1-12.

Yao, Y.; Guo, D. L.; Yao, S. B.; Yang, G. W. (2012)**:** Unsteady aerodynamic characteristics analysis of high speed pantograph. *Computer Aided Engineering*, vol. 21, no. 5, pp. 1-5.

Li, T.; Zhang, J. Y.; Rashidi, M.; Yu, M. G. (2019): On the Reynolds-averaged Navier-Stokes modeling of the flow around a simplified train in crosswinds. *Journal of Applied Fluid Mechanics*, vol. 12, no. 2, pp. 551-563.

Li, T.; Hemida, H.; Zhang, J. Y.; Rashidi, M.; Flynn, D. (2018)**:** Comparisons of shear stress transport and detached eddy simulations of the flow around trains. *Journal of Fluids Engineering*, vol. 140, no. 11, pp. 111108-111112.